

Quantum conductance of carbon nanotubes with defects

Leonor Chico,* Lorin X. Benedict, Steven G. Louie, and Marvin L. Cohen

Department of Physics, University of California at Berkeley, Berkeley, California 94720 and Materials Sciences Division, Lawrence Berkeley Laboratory, Berkeley, California 94720

(Received 11 March 1996)

We study the conductance of metallic carbon nanotubes with vacancies and pentagon-heptagon pair defects within the Landauer formalism. Using a tight-binding model and a Green's function technique to calculate the scattering matrix, we examine the one-dimensional to two-dimensional crossover in these systems and show the existence of metallic tube junctions in which the conductance is suppressed for symmetry reasons. [S0163-1829(96)00125-7]

I. INTRODUCTION

Since their discovery in 1991 by Iijima,¹ carbon nanotubes have attracted much attention. One of the most fascinating aspects of these systems is that their electronic properties are directly and sensitively related to their geometry. Carbon nanotubes can be metallic or semiconducting, depending on how the graphite sheet is rolled up to form the tube. The geometrical structure is uniquely determined by the circumference vector, $\mathbf{c} = n\mathbf{a}_1 + m\mathbf{a}_2$, where \mathbf{a}_1 and \mathbf{a}_2 are graphite sheet lattice translation vectors.² The ordered pair (n, m) defines the radius and chirality of each tube.³ Tubes indexed by $(n, 0)$ or (n, n) are nonchiral, while others have hexagonal carbon rings, which are arranged in a helical fashion. All (n, n) so-called armchair nanotubes are metals, and (n, m) tubes with the radii $> 3.5 \text{ \AA}$ are semimetallic if $n - m$ is a nonzero multiple of three.^{2,4} The rest are semiconductors, with band gaps that scale roughly as the reciprocal of the tube radius.

The introduction of topological defects can change the chirality of nanotubes. The smallest possible defect in a hexagonal rolled lattice that changes its chirality without drastically altering the local curvature is a pentagon-heptagon pair.⁵⁻⁷ In fact, it is possible to join two perfect nanotubes (n, m) and $(n \pm d, m \mp d)$ by forming d pentagon-heptagon pairs in the interface between them.⁸ The resulting carbon nanotube heterojunction, $(n, m)/(n \pm d, m \mp d)$, can have a different electronic structure on each side of the interface.⁷ The heterostructures formed by joining nanotubes of different chirality may show unique quasi-one-dimensional transport properties.

There are theoretical and experimental studies on the quantum transport properties of carbon nanotubes in the literature. On the experimental side, the conductance of nanotube bundles has been measured,⁹ and a measurement of the conductance of an isolated multiwalled carbon nanotube has been recently reported.¹⁰ From the theoretical viewpoint, there are studies on the effect of magnetic fields and voltage bias in the ballistic conductance of perfect nanotubes,¹¹ using the Landauer approach,¹² but there have been no studies of changes in the conductance produced by vacancies or adjacent pentagon-heptagon pairs.¹³ We address this issue by calculating the conductance of metallic carbon nanotubes with such defects using the Landauer formula¹² in a tight-binding

scheme. Within the Landauer formalism, the ballistic conductance of perfect systems is proportional to the number of conducting channels at the Fermi energy, that is, the number of bands at this energy.¹⁴ The conductance of an imperfect system is lowered, due to reflection of the electron waves off the defects. We first study the simplest possible defect, a single vacancy, and calculate the conductance as a function of tube radius. The increase of conductance with radius illustrates the crossover from one-dimensional to two-dimensional behavior. We then calculate the conductance through nanotube heterojunctions, $(n_1, m_1)/(n_2, m_2)$, where both (n_1, m_1) and (n_2, m_2) tubes are metallic. We show that certain configurations of the pentagon-heptagon pair defects completely stop the flow of electrons, while others permit the transmission of the current through the interface. Such systems may be used as nanoscale electrical switches.

The paper is organized as follows: in Sec. II, we introduce the model and method employed. Results are presented in Sec. III. Section IV contains a discussion of our findings. We conclude in Sec. V.

II. MODEL AND METHOD

We are interested in studying infinitely long carbon nanotubes with localized defects. First, we consider the problem of a vacancy in an otherwise perfect tube. We also study nanotubes with pentagon-heptagon pairs, which can be viewed as the result of matching two perfect semi-infinite tubes with different chiralities. This kind of problem is most conveniently treated with the Green's function matching (GFM) method.¹⁵ A nanotube with pentagon-heptagon pairs is depicted schematically in Fig. 1. The perfect tubes are media A and B. The last unit cell of medium A, labeled -1 , together with the first of medium B, labeled 1, consti-

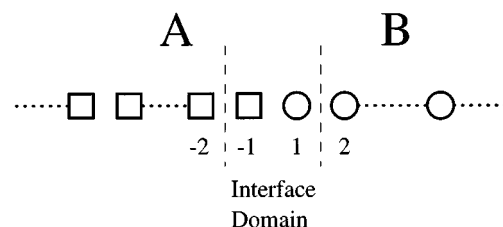


FIG. 1. Schematic view of a matched A|B system.

tute the interface domain. We describe the carbon nanotubes by a tight-binding model with one π -electron per atom. Our tight-binding Hamiltonian is of the form

$$H = -V_{pp\pi} \sum_{\langle ij \rangle} a_i^\dagger a_j + \text{c.c.}, \quad (1)$$

where the sum in i, j is restricted to nearest-neighbor atoms, and $V_{pp\pi} = 2.66$ eV, as in Ref. 7. On-site energies are set to zero. All the hopping parameters are equal, independent of the bond length, curvature, or any rearrangement due to the presence of defects. Therefore, our results show the changes induced solely by the alterations in the topology of the hexagonal rolled lattice. A vacancy is simulated by setting the hoppings to zero around the vacant site and its on-site energy equal to a large value, so the impurity peak does not appear in the energy range for which the density of states (DOS) of the tube is nonzero. We now describe the salient features of the GFM, and show how it is applied to calculate the conductance.

A. The Green's function matching method

In the GFM method, the single-particle Green's function of the tube with pentagon-heptagon pairs, G , is calculated from the bulk Green's functions and Hamiltonians of the perfect, defect-free systems, G_A , G_B , H_A , and H_B , respectively, and the coupling interaction between media A and B . This method can be used with different one-electron Hamiltonian models.¹⁵ Within the tight-binding model we employ, the Hamiltonians and the Green's functions are matrices, the dimensions of which are $(N_c N_e) \times (N_c N_e)$, where N_c is the number of unit cells and N_e is the number of π electrons/cell. Since we are studying infinite systems, in principle, these matrices are infinite. An element of G would be denoted by $\langle i, \alpha | G | j, \alpha' \rangle$, where i, j are cell indices and α, α' denote orbitals. In what follows, we let $H_{Mi,j}$ denote the *block* of the Hamiltonian matrix of the perfect system M ($M=A, B$), which contains matrix elements of H_M between localized π -electron orbitals in cell i and orbitals in cell j . Thus, $H_{Mi,j}$ is itself a matrix of dimension $N_{Me} \times N_{Me}$ (similarly for $G_{Mi,j}$). Using the GFM, we will only have to deal with block matrices, the dimensions of which are at most $(N_{Ae} + N_{Be}) \times (N_{Ae} + N_{Be})$, N_{Ae} and N_{Be} being the number of orbitals per cell in materials A and B , respectively.

The coupling between media A and B is given by the block matrices $H_{I-1,1}$ and $H_{I1,-1}$. $H_{I-1,1}$ contains matrix elements between orbitals in cells -1 and 1 . Obviously $H_{I1,-1} = H_{I-1,1}^\dagger$. The dimension of $H_{I-1,1}$ is $N_{Ae} \times N_{Be}$, so, in general, it is a rectangular matrix.

From G , we can evaluate the local density of states $N_n(E)$ at any energy E and n th cell of the system,

$$N_n(E) = -\frac{1}{\pi} \text{Im tr } G_{n,n}(E), \quad (2)$$

where the trace is over the N_e orbitals in cell n .

The total Green's function, G , is calculated in the following way: Suppose that in our matched system, $A|B$, we have an incident amplitude from side A , and we want to know the amplitude produced by the scattering at the interface. That is,

given an excitation in cell n of medium A propagating toward the interface, we are interested in knowing the amplitude produced in cell n' of medium B (transmission) or medium A (reflection).

In the first case, i.e., for transmission amplitudes, we have that

$$G_{n,n'} = G_{Bn,1} \mathcal{G}_B^{-1} \mathcal{G} \mathcal{G}_A^{-1} G_{A-1,n'}, \quad (3)$$

where calligraphic letters indicate interface objects, e.g., \mathcal{G} is the Green's function of the system projected onto the interface domain. For reflected amplitudes, we have

$$G_{n,n'} = G_{Mn,n'} + G_{Mn,-1} \bar{\mathcal{G}}_M^{-1} (\mathcal{G} - \mathcal{G}_M) \bar{\mathcal{G}}_M^{-1} G_{M-1,n'}, \quad (4)$$

where we have written the Green's function separating the incident and reflected part; the second term in Eq. (4) accounts for reflection at the interface. This will be useful for deriving an expression for the scattering matrix within the Green's function scheme.

For computational purposes, it is convenient to introduce the transfer matrices of medium M , T_M , S_M , \bar{T}_M , \bar{S}_M ,¹⁵ as

$$G_{Mn+1,m} = T_M G_{Mn,m}, \quad (n \geq m), \quad (5)$$

$$G_{Mn-1,m} = \bar{T}_M G_{Mn,m}, \quad (n \leq m), \quad (6)$$

$$G_{Mn,m+1} = G_{Mn,m} S_M, \quad (m \geq n), \quad (7)$$

$$G_{Mn,m-1} = G_{Mn,m} \bar{S}_M, \quad (m \leq n). \quad (8)$$

We compute the transfer matrices using the algorithm of L3pez Sancho *et al.*¹⁶ From Eqs. (5)–(8), it is easily seen that

$$\bar{S}_M = \bar{\mathcal{G}}_M^{-1} T_M \mathcal{G}_M, \quad (9)$$

$$S_M = \mathcal{G}_M^{-1} \bar{T}_M \mathcal{G}_M, \quad (10)$$

so that we only need to calculate two of the four transfer matrices defined above. Nevertheless, we maintain all four to yield more compact expressions. Using the former definitions, it can be shown that¹⁵

$$\mathcal{G} \equiv \begin{pmatrix} \mathcal{G}_{BB} & \mathcal{G}_{BA} \\ \mathcal{G}_{AB} & \mathcal{G}_{AA} \end{pmatrix} = \begin{pmatrix} E - H_{B1,1} - H_{B1,2} T_B & H_{I1,-1} \\ H_{I-1,1} & E - H_{A-1,-1} - H_{A-1,-2} T_A \end{pmatrix}^{-1}. \quad (11)$$

The full Green's function matrix, G , can then be constructed from Eqs. (3) and (4).

B. Scattering matrix and conductance

In the Landauer formalism, the conductance of a system is related to its scattering properties,¹² which are described using the Green's function scheme presented in the previous subsection. The multichannel generalization of the Landauer conductance formula is¹⁴

$$\Gamma = \frac{2e^2}{h} \text{Tr} (t^\dagger t) = \frac{2e^2}{h} \sum_{\beta\alpha} |t_{\beta\alpha}|^2, \quad (12)$$

where t is the transmission matrix from either the left or the right, as defined by Fisher and Lee. Let us choose the transmission from left to right, i.e., from medium A to B . Sup-

pose that at the energy E there are M_A channels in medium A and M_B channels in medium B . Then t is a rectangular $M_B \times M_A$ matrix. The squared modulus of a component of t , $|t_{\beta\alpha}|^2$, is the transmission coefficient from channel α in medium A to channel β in medium B . If we have an incident eigenstate from medium A , φ_α , the corresponding transmitted amplitude in side B , ψ_{asc} , can be written as a linear combination of the eigenstates of medium B , φ_β , provided that we are far from the interface. So $|t_{\beta\alpha}|^2 = v_\beta/v_\alpha |\langle \varphi_\beta | \psi_{\text{asc}} \rangle|^2$, where v_β, v_α are the group velocities of the corresponding eigenstates.

The scattered wave, ψ_{asc} , is calculated from the scattering matrix, $S(E)$, which is defined by

$$\begin{pmatrix} \Psi_{B,\text{out}} \\ \Psi_{A,\text{out}} \end{pmatrix} = S(E) \begin{pmatrix} \Psi_{B,\text{in}} \\ \Psi_{A,\text{in}} \end{pmatrix}, \quad (13)$$

where $\Psi_{\text{in}}, \Psi_{\text{out}}$ denote the ingoing and outgoing wave function amplitudes, respectively. The transmitted amplitude is obtained by setting Ψ_{in} equal to an incident eigenstate. Using the relation between the wave function amplitudes and the Green's function,¹⁵ we can write the scattering matrix in terms of \mathcal{G} : For example, the reflected amplitude in medium B is

$$\Psi_n = \varphi_{Bn} + G_{Bn,1} \mathcal{G}_B^{-1} (\mathcal{G}_{BB} - \mathcal{G}_B) \mathcal{G}_B^{-1} G_{B-1,n'} G_{Bn',n'}^{-1} \varphi_{Bn'}, \quad (14)$$

where φ_B is an incident eigenstate in medium B . Similarly, for the amplitude transmitted from side A to B ,

$$\Psi_n = G_{Bn,1} \mathcal{G}_B^{-1} \mathcal{G}_{BA} \mathcal{G}_A^{-1} G_{A-1,n'} G_{An',n'}^{-1} \varphi_{An'}, \quad (15)$$

and so on. Using (5)–(8), we can write the scattering matrix $S(E)$ as

$$\begin{aligned} S(E) &\equiv \begin{pmatrix} S_{BB} & S_{BA} \\ S_{AB} & S_{AA} \end{pmatrix} \\ &= \begin{pmatrix} T_B^{n'} & 0 \\ 0 & \bar{T}_A^n \end{pmatrix} \begin{pmatrix} \mathcal{G}_{BB} - \mathcal{G}_B & \mathcal{G}_{BA} \\ \mathcal{G}_{AB} & \mathcal{G}_{AA} - \mathcal{G}_A \end{pmatrix} \begin{pmatrix} S_B^{n'} & 0 \\ 0 & \bar{S}_A^n \end{pmatrix} \\ &\quad \times \begin{pmatrix} G_{Bn',n'}^{-1} & 0 \\ 0 & G_{An,n}^{-1} \end{pmatrix}. \end{aligned} \quad (16)$$

If we take n, n' far from the interface, we can choose the incident amplitudes as eigenstates of the unperturbed Hamiltonian H_A , and decompose the scattered wave functions in terms of the eigenstates of the unperturbed Hamiltonian H_B . Thus, in terms of the scattering matrix, Eq. (12) reads

$$\Gamma(E) = \frac{2e^2}{h} \sum_{\alpha\beta} \left(\frac{v_\beta}{v_\alpha} \right) |\langle \varphi_\beta | S_{BA}(E) | \varphi_\alpha \rangle|^2, \quad (17)$$

where the indices α, β run over all eigenstates with energy E of media A and B , respectively.

III. RESULTS

A. Carbon nanotubes with vacancies

In this section, we study the conductance of several (n,n) carbon nanotubes in which an atom has been removed to produce a vacancy. In Fig. 2, we plot the conductance of

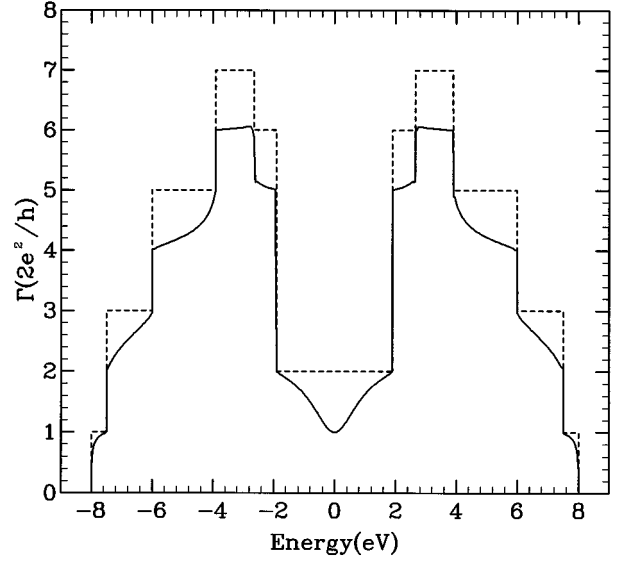


FIG. 2. Conductance of a $(4,4)$ nanotube with a vacancy (full line) and a perfect $(4,4)$ nanotube (dashed line) as a function of the Fermi energy.

the $(4,4)$ nanotube with one vacancy (full line) and the perfect $(4,4)$ tube (dashed line) as a function of the energy. For most energies, and particularly at the Fermi energy of the undoped system ($E=0$), the value of the conductance is reduced by almost one unit, $2e^2/h$, when the impurity is present. This amounts to the removal of one conducting channel, and for the undoped case, a reduction of 50% with respect to the conductance of the perfect $(4,4)$ nanotube. This is to be expected, for the presence of a vacancy in a monatomic chain completely suppresses the conductance by removing the only existing channel. Since a nanotube is a *quasi*-one-dimensional system, the conductance is not totally suppressed; the extent to which it is depleted reflects the dimensionality of the system.

Figure 3 shows the difference between the conductance (for $E_F=0$) of a perfect (n,n) tube and that of the same tube with a vacancy as a function of n . The circumference of an (n,n) tube is given by $C=3nl$, where l is the carbon-carbon nearest-neighbor distance, so this is equivalent to plotting the change in conductance versus nanotube radius. All perfect (n,n) tubes have two bands at E_F , giving rise to a conductance of $4e^2/h$. When the impurity is introduced, the conductance decreases, this decrease being greater for the smaller tubes. Note that for the $(4,4)$ tube the conductance is reduced by one channel, and this difference diminishes smoothly when the radius increases. An increase in radius corresponds to a change from quasi-one-dimensional to two-dimensional behavior. In a perfect two-dimensional graphite sheet the change in conductance, due to the presence of a single vacancy, is negligible.

B. Pentagon-heptagon matched tubes: Nanotube heterojunctions

We now come to the main focus of this work, the conductance of matched metallic carbon tubes with pentagon-heptagon pair defects. First, we study the $(12,0)/(6,6)$ tube.

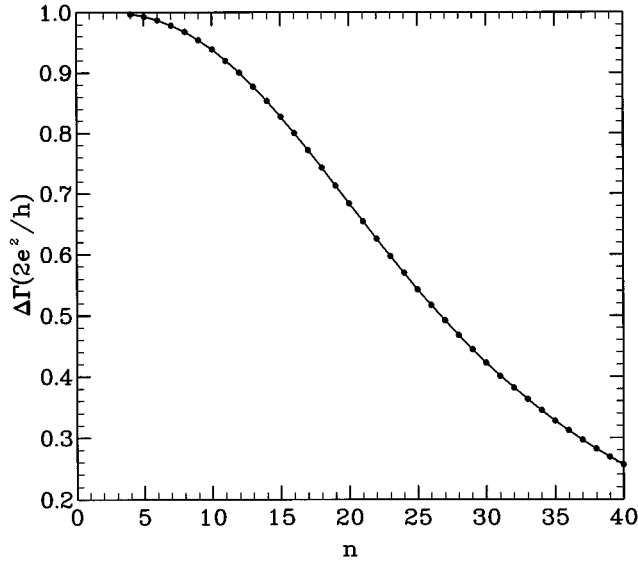


FIG. 3. The difference in the conductance of an (n,n) nanotube with and without a vacancy as a function of n .

There is a unique way to match these two tubes by joining their perfect unit cells, which produces a ring of six pentagon-heptagon pairs around the circumference. In Fig. 4 (top), we show the conductance of the matched tube together with the conductances of the $(12,0)$ and $(6,6)$ perfect tubes as a function of energy. We see that, whereas the perfect tubes are metallic and have a nonzero conductance at the Fermi energy of the undoped tube ($E_F=0$), there is a gap in the conductance for the matched system. The conductance of the matched tube is always smaller than the conductance of the perfect tubes that form it, as expected: any defect degrades the conductance, and in a matched system $A|B$ medium B can be considered as a perturbation to medium A and vice versa. This effect is similar to what Todorov and Briggs¹⁷ noted studying the conductance of wires with width fluctuations. In Fig. 4 (center) and 4 (bottom), we present the local density of states (LDOS) of the unit cells, which contain the pentagon-heptagon pairs (full lines).¹⁸ In our notation, these are cells with $n = -1$ [for the $(12,0)$ tube, Fig. 4, center] and $n = 1$ [for the $(6,6)$ tube, Fig. 4, bottom]. For comparison, we also plot the LDOS of the perfect tubes [dotted line in Fig. 4 (center) and dashed line in Fig. 4 (bottom), respectively]. The LDOS is nonzero in the defect region for the energy interval in which the conductance is zero, as it is for the perfect tubes. Therefore, the conductance is not suppressed, due to the appearance of a gap in the LDOS in the defect region. This points to a symmetry origin of the suppression of the conductance in this system. We discuss this at length in the following section. One may wonder whether the presence of a full ring of pentagon-heptagon pairs around the circumference of the tube could be related to this effect.

To clarify this point, we have studied a tube for which the matching is achieved by a mixture of hexagons and pentagon-heptagon pairs, the $(9,0)/(6,3)$ tube. In this case, three pentagon-heptagon pairs are needed, so the matching region contains three hexagons as well. There are several inequivalent ways of joining the perfect unit cells: all the hexagons adjacent to each other, only two of the hexagons adjacent, and all the hexagons separated. Here, we study two

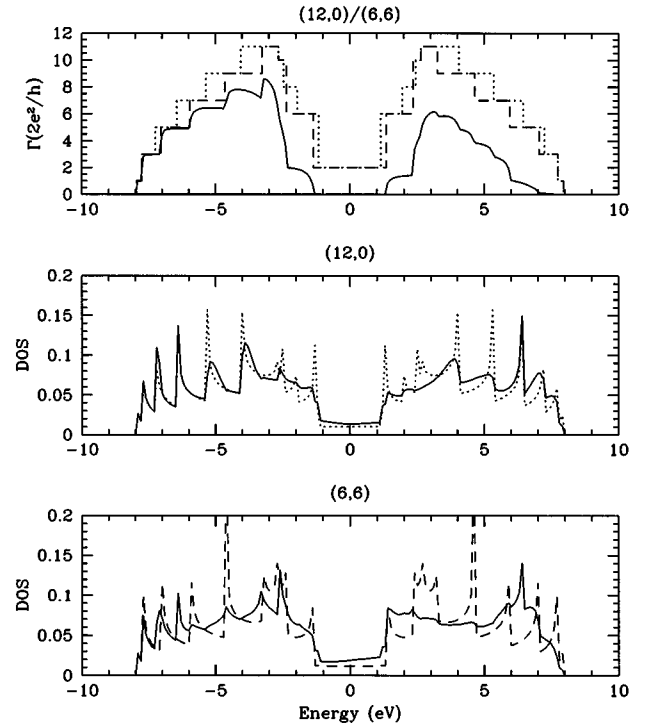


FIG. 4. Results for the $(12,0)/(6,6)$ matched tube. Top: conductances of the matched system (solid line), perfect $(12,0)$ tube (dashed line), and perfect $(6,6)$ tube (dotted line). Center: atom-averaged LDOS of the interface unit cell of the $(12,0)$ tube (full line) and the perfect $(12,0)$ tube (dotted line), plotted for comparison. Bottom: atom-averaged LDOS of the interface unit cell of the $(6,6)$ tube (full line) and the perfect $(6,6)$ tube (dashed line), plotted for comparison.

of these possible matching orientations: (1) symmetric: all the hexagons separated by defects, and (2) asymmetric: two hexagons adjacent to each other. The first is so named because the sequence of n -fold atom rings around the circumference (6-7-5-6-7-5-6-7-5) has threefold rotational symmetry about the cylindrical axis of the tube. The asymmetric case has no rotational symmetry (sequence of n -fold rings is 6-7-5-6-6-7-5-7-5).

In Fig. 5, we present the results for the $(9,0)/(6,3)$ symmetric tube. Figure 5 (top) shows the conductance along with the conductance of its perfect components, i.e., the $(9,0)$ (dashed line) and the $(6,3)$ (dotted line). Again, we find that there is a gap in the conductance around the Fermi energy of the undoped system, so that the appearance of a conductance gap is not exclusive to tubes with a full circumference of pentagon-heptagon pairs. As before, the conductance of the matched tube is lower at every energy than that of its perfect constituents. In Fig. 5 (center) and 5 (bottom), we show the LDOS of the matched unit cells that form the interface (full lines) along with the LDOS of the corresponding perfect $(9,0)$ and $(6,3)$ tubes (dashed and dotted lines, respectively). Again the LDOS is nonzero in the energy interval in which the conductance is zero.

The results for the asymmetric $(9,0)/(6,3)$ tube are shown in Fig. 6. For this tube, we find that there is not a total suppression of the conductance at any energy at which the LDOS is nonzero (Fig. 6, top, full line): the matched system

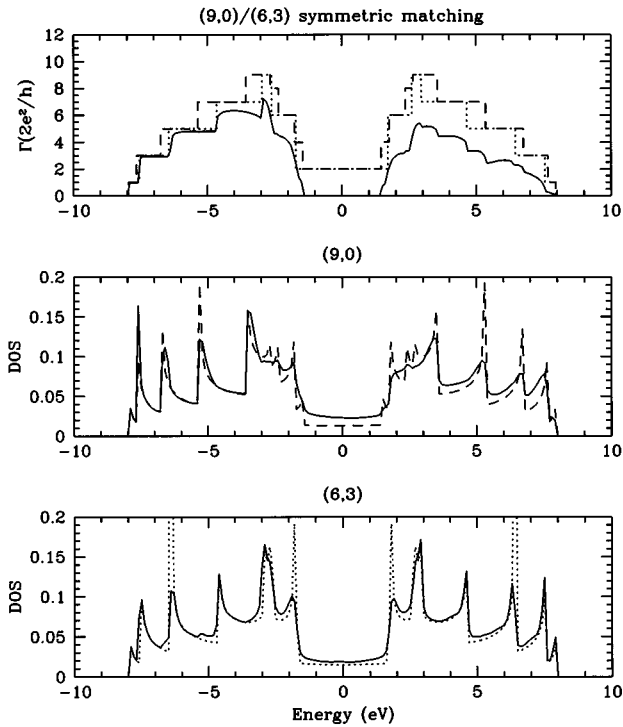


FIG. 5. Results for the (9,0)/(6,3) symmetric matched tube. Top: conductances of the matched system (solid line), perfect (6,3) tube (dotted line), and perfect (9,0) tube (dashed line). Center: atom-averaged LDOS of the interface unit cell of the (9,0) tube (full line) and the perfect (9,0) tube (dashed line), plotted for comparison. Bottom: atom-averaged LDOS of the interface unit cell of the (6,3) tube (full line) and the perfect (6,3) tube (dotted line), plotted for comparison.

behaves as a metal. Nevertheless, since the interface between the tubes acts as a defect, the conductance is reduced by approximately one channel relative to that of the perfect tubes. As in the previous cases, we plot the conductances of the (9,0) and (6,3) perfect tubes for comparison. The LDOS at the interface (Fig. 6, center and bottom, full lines) is practically equal to the one found for the symmetric case (see Fig. 5). The rest of the features are very similar to the symmetric case. The metallic nature of the asymmetric (9,0)/(6,3) tube provides further evidence that the presence of a conductance gap is related to the symmetry of the defects at the interface. In what follows, we explain this effect and derive general rules that predict the occurrence of conductance gaps in $(n_1, m_1)/(n_2, m_2)$ systems.

IV. DISCUSSION

We first explain the conductance gap in the (12,0)/(6,6) tube. A discussion of the (9,0)/(6,3) system and the general rules for all the $(n_1, m_1)/(n_2, m_2)$ tubes follow. If curvature-induced hybridization is neglected,⁴ carbon nanotubes can be thought of as graphite sheets with periodic boundary conditions applied in the circumferential direction. This results in a quantization of allowed \mathbf{k} vectors of the graphite sheet, which forms the tube.² Figure 7 shows the lines of allowed \mathbf{k} vectors overlayed on the graphite sheet first Brillouin zone (BZ) for the perfect (6,6) and (12,0) tubes. Both tubes have

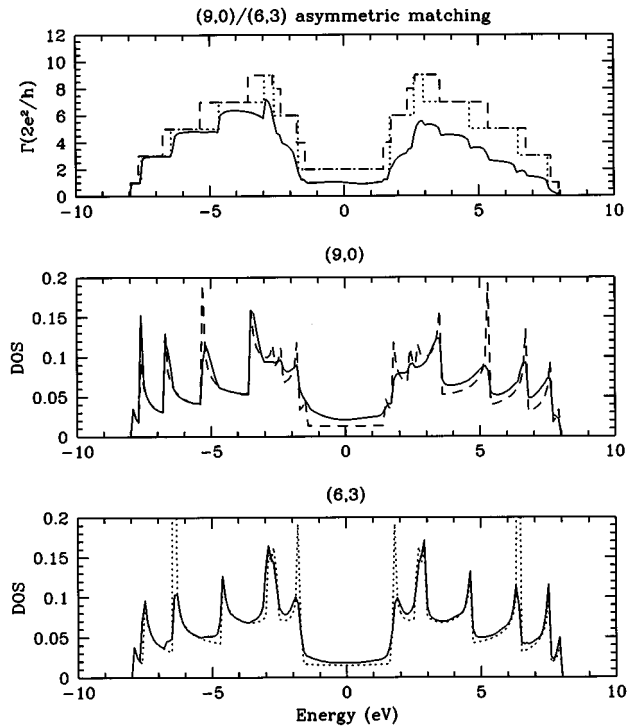


FIG. 6. Results for the (9,0)/(6,3) asymmetric matched tube. Top: conductances of the matched system (solid line), perfect (6,3) tube (dotted line), and perfect (9,0) tube (dashed line). Center: atom-averaged LDOS of the interface unit cell of the (9,0) tube (full line) and the perfect (9,0) tube (dashed line), plotted for comparison. Bottom: atom-averaged LDOS of the interface unit cell of the (6,3) tube (full line) and the perfect (6,3) tube (dotted line), plotted for comparison.

sixfold rotational symmetry about their cylindrical axes. Thus, electronic states of the tubes may be classified according to discrete angular momenta L .¹⁹ States that arise from different lines of allowed \mathbf{k} vectors have different rotational symmetries. The lines that intersect $\mathbf{k}=0$ give rise to rotationally invariant ($L=0$) tube states. Other lines give rise to states of higher L .

The states with energies near E_F (for the undoped case) are those with \mathbf{k} vectors close to the vertices of the hexago-

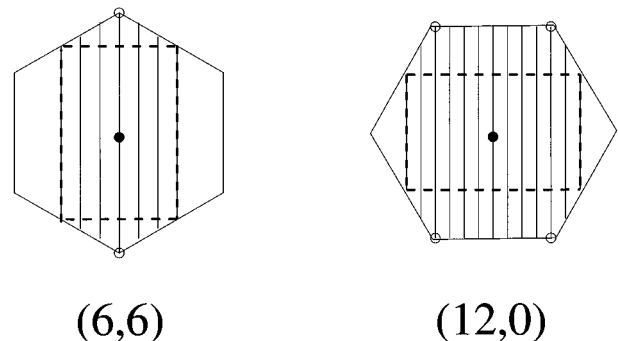


FIG. 7. Lines of allowed \mathbf{k} vectors of the (6,6) and (12,0) carbon nanotubes overlayed on the graphite sheet Brillouin zone. Dashed lines enclose Brillouin zones of the (1,1) and (1,0) units. Solid dots indicate $\mathbf{k}=0$, and open dots mark points where the lines touch the graphite sheet Fermi surface.

nal BZ.² This is because the Fermi surface of the undoped graphite sheet is located at these points. Thus, the states at E_F for the (6,6) tube originate from the center line, and are $L=0$ states, invariant under rotations by $2\pi/6$ about the tube axis. The Fermi level states of the (12,0) tube come from the fourth line away from the center, and are $L=2$ states (defined with respect to sixfold rotational symmetry). So we see that the Fermi level states of the two perfect tubes have *different rotational symmetries*.

When the two tubes are matched to form the junction, (12,0)/(6,6), six pentagon-heptagon pairs are introduced at the interface. The interface itself has sixfold rotational symmetry. Therefore, the matched tube is invariant under rotations by $2\pi/6$. Now consider the conduction process. Scattering due to rigid defects is elastic as long as the defects have no internal excitations. Thus, an electron which begins in the (12,0) tube must scatter to a state with the same energy in the (6,6) tube. But since the states at E_F of the two half tubes have different L , the electron wave is *totally reflected*, and the conductance equals zero. Stated another way, the perfectly symmetric interface cannot impart any extra angular momentum to the electron, so the conditions of energy and angular momentum conservation cannot be satisfied simultaneously.²⁰ If the system is doped with either electrons or holes, such that E_F is pushed away from 0 to energies at which states of equal L coexist on both halves of the junction, the conductance is nonzero. The conductance gap marks the energy window in which states of the two sides have no L values in common.

It should be pointed out that the $L=0$ states of the (6,6) side of the junction do extend into the (12,0) side, but they decay away from the interface, as is typical of interface states. Likewise, the $L=2$ states of the (12,0) side extend into the (6,6) side, but are damped. Since evanescent waves carry no current, the resulting conductance is zero. This is similar to the total reflection in wave optics: even when the reflectance equals unity, some nonzero amplitude penetrates. However, far from the reflecting surface (on the opposite side from the source), no light flux is measured.

The above arguments may also be applied to the (9,0)/(6,3) system. Consider the symmetric matching case. The interface (6-7-5-6-7-5-6-7-5) has threefold rotational symmetry about the tube axis, as do the individual (9,0) and (6,3) tubes. From the graphite sheet band-folding analysis, it can be shown that the states at E_F for the (6,3) tube have $L=1$ (defined with respect to threefold rotational symmetry). The Fermi level states of the (9,0) tube have $L=0$. Again, states on opposite sides of the interface have different rotational symmetries. The symmetric interface does not impart extra angular momentum to the conducting electrons, so there is a conductance gap near $E_F=0$.

Now consider the asymmetric matching case. The interface (6-7-5-6-6-7-5-7-5) has *no* rotational symmetry whatsoever, and in particular, it lacks threefold symmetry. Therefore, transitions between the $L=1$ states of the (6,3) side, and the $L=0$ states of the (9,0) side are permitted; the interface can impart angular momentum to the electron. This results in a conductance which is nonzero over the whole energy range where the DOS is nonzero.

A general rule can now be abstracted: Carbon nanotube heterojunctions may have conductance gaps if the defects

that form the interface are arranged symmetrically. They will not have conductance gaps if the interface does not preserve the rotational symmetry of the two constituent tubes. Of course, it is possible to match two tubes with different rotational symmetries.²¹ In this case, no symmetric matching is possible, and conductance gaps will never appear. It is also possible for symmetrically matched tubes to avoid having a conductance gap. This will happen when the states of the two sides have some L values in common at every energy.

We can easily derive the necessary condition on n_1, m_1, n_2 , and m_2 , such that the $(n_1, m_1)/(n_2, m_2)$ matched tube is a candidate for a conductance gap: An (n, m) tube has J -fold rotational symmetry if n and m are both divisible by J . Thus, if n_1, m_1, n_2 , and m_2 all have a common divisor, it will be possible to form the $(n_1, m_1)/(n_2, m_2)$ junction with a rotationally symmetric interface. A conductance gap may result. Otherwise the conductance will, in general, be nonzero in the energy range for which the DOS is nonzero. Note that even if the two constituent tubes share a common rotational symmetry, it is usually possible to choose an asymmetric matching [see the asymmetric (9,0)/(6,3) above]. A conductance gap can then be avoided [it cannot be avoided in the (12,0)/(6,6) system with ideal unit cell matching]. It should be mentioned that the above argument holds for all types of defects at the interface. Only the symmetry of the interface is relevant.

One point of interest is the variation in geometrical structure of carbon nanotube heterojunctions with different matching configurations. Nanotubes with pentagon-heptagon pair defects may exhibit localized kinks and bends. Bend angles of up to 15° have been predicted,^{5,7} and tubes with these signatures have been seen experimentally.⁵ A nanotube heterojunction with a bend is the result of an asymmetric matching at the interface; rotational invariance is destroyed. If two tubes are matched symmetrically, the junction will have no bend, for the axis of rotational symmetry is preserved. Thus, there is a relationship between the geometry of nanotube heterojunctions and the appearance of conductance gaps. Bent junctions will, in general, have a nonzero conductance if the constituent tubes are metallic. Straight junctions may have conductance gaps. So we have the somewhat counterintuitive result that bent junctions conduct better than straight junctions on average.

The presence of conductance gaps in some carbon nanotube heterojunctions opens up new possibilities for their potential applications. Since conductance gaps arise from a rotational symmetry, any perturbation that destroys this symmetry will allow the tube to conduct. Three sources of symmetry breaking are thermally excited phonons, externally applied electromagnetic (EM) radiation, and mechanical deformation. If a nanotube heterojunction with a conductance gap is at very low temperature, only acoustic phonon modes with $\mathbf{q} \sim 0$ will be excited. From the above band-folding analysis, these modes will be symmetric ($L=0$), and will not change the rotational symmetry of the interface. If the junction is at slightly higher temperature, asymmetric phonon modes ($L>0$) will be excited, which break the rotational symmetry, and destroy the conductance gap. The conductance should then show a sharp increase as temperature is increased. Therefore, heterojunctions with conductance gaps may be used as nanoscale thermistors, which operate in the

10–100 K range. Heterojunctions kept at low temperature may lose their conductance gaps when bathed with appropriately polarized EM radiation. Circularly polarized photons with \mathbf{E} fields rotating about the tube axis can impart angular momentum to the conduction electrons. This allows the electrons to cross the interface and conduct current. Thus, these systems could also be used as nanoscale photoconductive switches that operate over a wide range of frequencies (unlike typical photoconductive materials, it is the exchange of angular momentum rather than energy that excites the electrons into conducting states). Finally, mechanical stress can be used to destroy the rotational symmetry of a junction. If a nanotube heterojunction is anchored at both ends, a nanoscale piezoelectric particle positioned alongside the interface may deform the tube wall enough to allow the flow of current. In this way, heterojunctions could be used as nanoscale voltage-activated electrical switches.

V. CONCLUSION

We have studied the conductance of metallic carbon nanotubes with defects using the Landauer approach and a tight-binding Green's function technique. We find that a single vacancy produces a dramatic decrease in the conductance of small-radius tubes, while tubes with large radii are

less affected. This is indicative of the crossover from one-dimensional to two-dimensional behavior. We have shown that carbon nanotube heterojunctions formed from two metallic tubes conduct if the defects at the interface are arranged asymmetrically. If the defects preserve the rotational symmetries of the two tubes, conductance gaps appear. Consequently, bent junctions conduct better than straight junctions on average. Owing to their novel properties, carbon nanotube heterojunctions with conductance gaps may be used as nanoscale thermistors, as well as optically activated and voltage-activated electrical switches.

ACKNOWLEDGMENTS

We are indebted to Dr. Jorge Iribas Cerdá, who spent long hours helping us clarify the subtleties of the multichannel conductance problem. This work was supported by the National Science Foundation Grant No. DMR-9520554 and by the Director, Office of Energy Research, Office of Basic Energy Sciences, Materials Sciences Division of the U.S. Department of Energy under Contract No. DE-AC03-76SF-00098. L. C. acknowledges the support of the Spanish Ministerio de Educación y Ciencia and S. G. L. acknowledges the support of the Miller Institute for Basic Research in Science.

*Present address: Instituto de Ciencia de Materiales de Madrid, Consejo Superior de Investigaciones Científicas, Cantoblanco, 28049 Madrid, Spain.

¹S. Iijima, *Nature* **354**, 56 (1991).

²R. Saito, M. Fujita, G. Dresselhaus, and M. S. Dresselhaus, *Appl. Phys. Lett.* **60**, 2204 (1992); N. Hamada, S. Sawada, and A. Oshiyama, *Phys. Rev. Lett.* **68**, 1579 (1992); J. M. Mintmire, B. I. Dunlap, and C. T. White, *ibid.* **68**, 631 (1992).

³Throughout this paper, we use the (n,m) notation of Saito *et al.* in Ref. 2.

⁴X. Blase, L. X. Benedict, E. L. Shirley, and S. G. Louie, *Phys. Rev. Lett.* **72**, 1878 (1994).

⁵T.W. Ebbesen and T. Takada, *Carbon* **33**, 973 (1995).

⁶Ph. Lambin, A. Fonseca, J. P. Vigneron, J. B. Nagy, and A. A. Lucas, *Chem. Phys. Lett.* **245**, 85 (1995). These authors consider carbon nanotubes with a pentagon and a heptagon on opposite sides of the tube perimeter. Thus, they consider tubes of a maximum bend angle, in contrast to the adjacent pentagon-heptagon minimum bend angle tubes that we study here.

⁷L. Chico, V. H. Crespi, L. X. Benedict, S. G. Louie, and M. L. Cohen, *Phys. Rev. Lett.* **76**, 971 (1996).

⁸Note that having d pentagon-heptagon (5-7) defects in a nanotube does not necessarily yield a $(n,m)/(n \pm d, m \mp d)$ junction. This happens when all the defects are not aligned with the tube axis and are not antiparallel. Actually, a 5-7/7-5 defect pair does not change the chirality of a nanotube at all. For an $(n,0)$ tube, one 5-7 defect aligned with the tube axis produces an $(n,0)/(n \pm 1,0)$ junction. We thank Dr. Vincent H. Crespi for pointing out this issue to us.

⁹S. N. Song, X. K. Wang, R. P. H. Chang, and J. B. Ketterson, *Phys. Rev. Lett.* **72**, 697 (1994); L. Langer, L. Stockman, J. P. Heremans, V. Bayot, C. H. Olk, C. Van Haesendonck, Y. Bruynseraede, and J.-P. Issi, *J. Mater. Res.* **9**, 927 (1994).

¹⁰L. Langer, V. Bayot, E. Grivei, J.-P. Issi, J. P. Heremans, C. H. Olk, L. Stockman, C. Van Haesendonck, and Y. Bruynseraede, *Phys. Rev. Lett.* **76**, 479 (1996).

¹¹W. Tian and S. Datta, *Phys. Rev. B* **49**, 5907 (1993); M. F. Lin and K. W. -K. Shung, *ibid.* **51**, 7592 (1995).

¹²R. Landauer, *Philos. Mag.* **21**, 863 (1970).

¹³There is a work in which the conductance of connected carbon nanotubes is calculated, R. Saito, G. Dresselhaus, and M. S. Dresselhaus, *Phys. Rev. B* **53**, 2044 (1996). However, in the cases studied by these authors the pentagon and heptagon are not adjacent.

¹⁴D. S. Fisher and P. A. Lee, *Phys. Rev. B* **23** 6851 (1981).

¹⁵F. García-Moliner and V. R. Velasco, *Theory of Single and Multiple Interfaces* (World Scientific, Singapore, 1992); M. C. Muñoz, V. R. Velasco, and F. García-Moliner, *Prog. Surf. Sci.* **26**, 117 (1987).

¹⁶M. P. López Sancho, J. M. López Sancho, and J. Rubio, *J. Phys. F* **14**, 1205 (1984); **15**, 851 (1985).

¹⁷T. N. Todorov and G. A. D. Briggs, *J. Phys. Condens. Matter* **6**, 2559 (1994).

¹⁸For each LDOS presented, we add the LDOS of all atomic sites in the cell, and divide by the number of atoms.

¹⁹We use the term “discrete angular momentum” somewhat loosely here. The more precise statement is that electronic states of n -fold rotationally symmetric tubes act as basis functions for irreducible representations of the point group C_n .

²⁰An approximate classical analog of this phenomenon can be found on pp. 85–86 of V. I. Arnold, *Mathematical Methods of Classical Mechanics* (Springer-Verlag, New York, 1989).

²¹See, for example, the $(8,0)/(7,1)$ junction studied in Ref. 7. In this case, however, the $(8,0)$ tube is a semiconductor, so the presence of a conductance gap is expected on more basic grounds.